μRheoSANS of Wormlike Micelle Solutions

Experiment Introduction

Viscoelastic wormlike micelles (WLMs) are important microstructures that relate to rheological properties of fluids in various applications ranging from fracture fluids in oil fields, drag reducing agents in district heating systems, home and personal care products to scaffolds for asymmetric and aligned nanostructures.[1] WLMs have also attracted numerous interest in fundamental research. Extensive work has been carried out to investigate the structures and dynamic properties of WLMs for various ionic surfactant types such as cationic, anionic, zwitterionic and different mixed ionic surfactant systems in aqueous media. [2] For ionic surfactant in aqueous media, at a surfactant concentration just above the critical micelle concentration (CMC), micelles are usually spherical in shape. The aggregate geometry may be predicted on the basis of critical packing parameter. The sphere-rod transition in the micellar shape can be induced in different ways such as increasing surfactant concentration, salinity or temperature, depending on the type of surfactant. Under certain conditions, some surfactant micelles exhibit enormous growth in one dimension and form very long and highly flexible aggregates, termed "wormlike" or "polymer-like" micelles. One-dimensional growth may be thermodynamically favorable for the system to minimize the excess free energy by reducing the number of rodlike micelle end caps without counteracting the entropy factor. Above the overlap concentration, the wormlike micelles entangled to form a transient network analogous to a polymer network, and exhibit viscoelastic behavior analogous to a flexible polymer solution. However, unlike polymers in solutions, WLMs undergo breaking and recombination, and, therefore, exhibit complex rheological behavior. [1, 2, 3]

In this experiment we will directly measure changes in the structure and rheology of wormlike micelle solutions that occur as a function of increasing flow rates. A model system of wormlike micelles in D_2O will be provided for the experiment. Instead of using traditional rheoSANS, we will utilize a microfluidic slit rheometer for simultaneous measurement of viscosity and structure. Analogous data from traditional (Couette) rheoSANS will be provided for comparison. μRheoSANS allows us to access much higher shear rates than accessible with traditional rheoSANS, but for this experiment we will focus primarily on studying the sample at shear rates accessible with both geometries. In addition to introducing the students to μRheoSANS, this experiment will also serve to facilitate a discussion of how to plan successful flowSANS experiments more generally and we will explain common ways that these experiments are expected to differ from more traditional SANS measurements.

Small-Angle Neutron Scattering (SANS)

Neutron scattering measures the change in momentum (mass and velocity) of the neutrons as they pass through the material and interact with nuclei. This change in momentum can reveal information about the structure (usually in elastic scattering) and motions within the material (typically seen in inelastic scattering). In contrast to x-ray scattering or visible light scattering, neutrons interact with the nuclei and not the electron cloud. As a result, neutrons often have very different interactions with a given material than those seen with electromagnetic radiation. This makes neutron scattering very complimentary to techniques that rely on electromagnetic scattering.

All neutron techniques interact with nuclei, however different techniques measure different properties of the neutron as they pass through the material. Small Angle Neutron Scattering (SANS) measures the elastic scattering function of the neutrons, meaning there is an inherent assumption that the neutrons have not lost energy (or changed wavelength) as they passed through the material. In most cases, this is a sufficient assumption. As in other forms of neutron scattering, SANS measures the change in momentum of the neutrons, where the momentum is defined as ½ m * **v**, m is the neutron mass and **v** is a vector of the neutron velocity (vectors are denoted here as boldface letters), In the assumption of elastic collisions, the magnitude of the m and **v** are constant. As a result, we are able to measure the momentum change, **Q**, by simply measuring the change in direction of the neutron upon scattering:

$$|\mathbf{Q}| = |\mathbf{k_o} - \mathbf{k_i}| = 4\pi/\lambda \sin(\theta) \qquad \text{(Eqn. 1)}$$

Here, the change in momentum is simply the difference in outgoing ($\mathbf{k_o}$) and incident ($\mathbf{k_i}$) momentums, and can be expressed using simple vector mathematics as an inverse function of wavelength (λ) and a trigonometric function of the half angle of scatter between the outgoing and incoming neutrons (θ). At small angles, note that $\sin(\theta) \sim \theta$. This relationship is often useful in back of the envelope estimates, however we will be using the full expression for our measurements. Since the wavelength is assumed constant, the SANS experiment is simply the measurement of scattered neutron intensity as a function of scattering angle at fixed wavelength, providing us with I(**Q**).

This data scattering as a function of Q is determined by measuring the neutrons that hit a detector located at some distance from the detector. By adjusting the sample to detector distance you can measure different q- ranges. In typical, static scattering experiments it is frequently expected that the samples will scatter isotropically – scattering with no apparent directionality – and in this case it is typical to take a circular average of the reduced data to make a 1D plot of differential scattering cross-section versus Q. However, in flowSANS, polarized beam measurements and in some other cases, it is often expected that there will be some sort of anisotropy in the scattering. An example of this would be in the scattering from wormlike micelles undergoing flow induced alignment. For anisotropic systems such as these, an alternate approach which takes into account scattering variation as a function of angle ϕ or direct analysis of the 2D data is required. In fact, one simple way to quantify alignment in these systems is to take an annular average about some limited q-range and plot the intensity as a function of ϕ. An even Legendre expansion can be used to fit this data and extract the Hermann orientation parameter.

Methods for Measurement Structure in Complex Fluids under Flow at the NCNR

Many complex fluids are known to exhibit either shear thinning, or thickening, under shear flow. This non-linear rheological behavior is typically tied directly to changes in the nanostructure of the material (Fig 1). Two examples of such complex fluids are dense colloidal suspensions (shear thickening) or wormlike micelle solutions (shear thinning). But similar flow behavior can be seen in many other complex fluids and are frequently utilized in commercial formulations. In

fact, in many cases a particular type of non-Newtonian fluid response may even be deliberately engineered, depending on the exact application. Over the last few decades, small angle neutron scattering has been used to directly measure scattering of complex fluids as they undergo flow induced structural transitions.

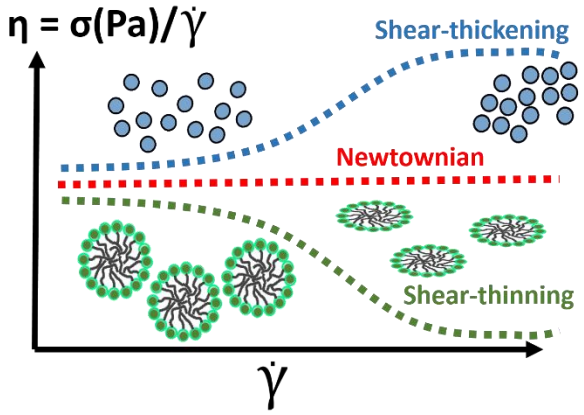

Figure 1: Many systems undergo structural changes under flow, which is strongly correlated to changes in their mechanical response.

One of the most frequently used and well established flowSANS techniques is rheoSANS. For these measurements, a rheometer is placed directly into the neutron beam, and scattering is collected simultaneously with the rheological data. Use of the rheometer rather than a flow cell both ensures high precision control of the shear field and simultaneous measurement of the sample rheology. The rheoSANS tool that is currently available in the user program is an Anton Paar rheometer with specially designed Couette geometries made from either quartz or titanium (owing to the relatively low interaction of neutrons with these materials). Furthermore, the temperature can be controlled between -40 and 200 °C. Shear rates as high as ~3,500 or ~10,000 s^{-1} can be achieved in low volume (~5-7 mL) and high volume 9~15 mL) geometries respectively. With this instrument, measurements can be made to probe the flow-vorticity or shear gradient-vorticity planes (radial or tangential measurements respectively).

Due to the physical constraints, both in terms of space and construction, rheoSANS measurements cannot be made in the flow-shear gradient (1-2 plane). However, purpose built devices, such as the 1-2 shear cell, can be used to measure in this orientation. [5] This device makes it possible to measure gap resolved structure, which is critical to understanding the structural origin of shear banding in some viscoelastic fluids. Furthermore, the alignment angle can be determined relative to the shear gradient only when measured in this orientation. It is important to note that the 1-2 shear cell is not a rheometer and no rheological data are collected during these experiments. [5]

Neither of these measurements can be made at very high shear rates (>10,000) as are frequently observed in industrial applications. An example of a high shear rate industrial application is the injection of pharmaceuticals through very small needles as shown in Figure 2. Achieving high shear rates approaching or exceeding 10^6 s^{-1}, however, will require as shift away from simple Couette flow. Capillary rheometers (diameters on the order of 10 – 100 μm) can be used to reach the desired shear rates, however such capillary devices are far too small to be effectively coupled to SANS measurements. Instead, we will use a microfluidic slit rheometer with very high aspect ratios (cross-sections on the order of 1 cm x 100 μm).

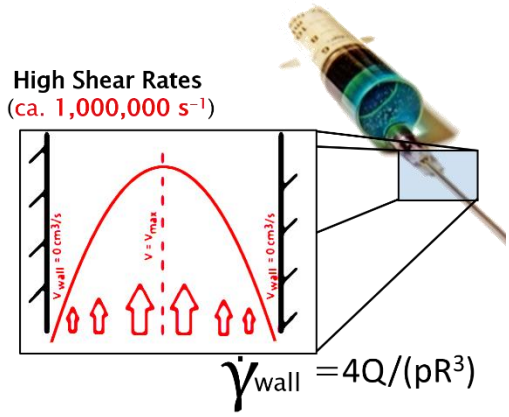

Figure 2: Industrial processing frequently requires pumping highly viscous fluids through narrow constrictions.

Design of Microfluidic Rheometer for High-Shear Rate RheoSANS (*μ*RheoSANS)

The behavior of complex fluids at conditions of high shear is of great interest across a number of otherwise disparate industries (Fig 2). Biological formulations, home care products, polymer melts, and a large number of other macromolecular or colloidal dispersions all display highly non-Newtonian flow behavior. Knowing the extent to which these fluids shear thin – or thicken, can be critical to predicting their behavior under processing conditions. Many applications require channeling fluid through narrow openings, as with injectables, hydraulic fracturing fluids,

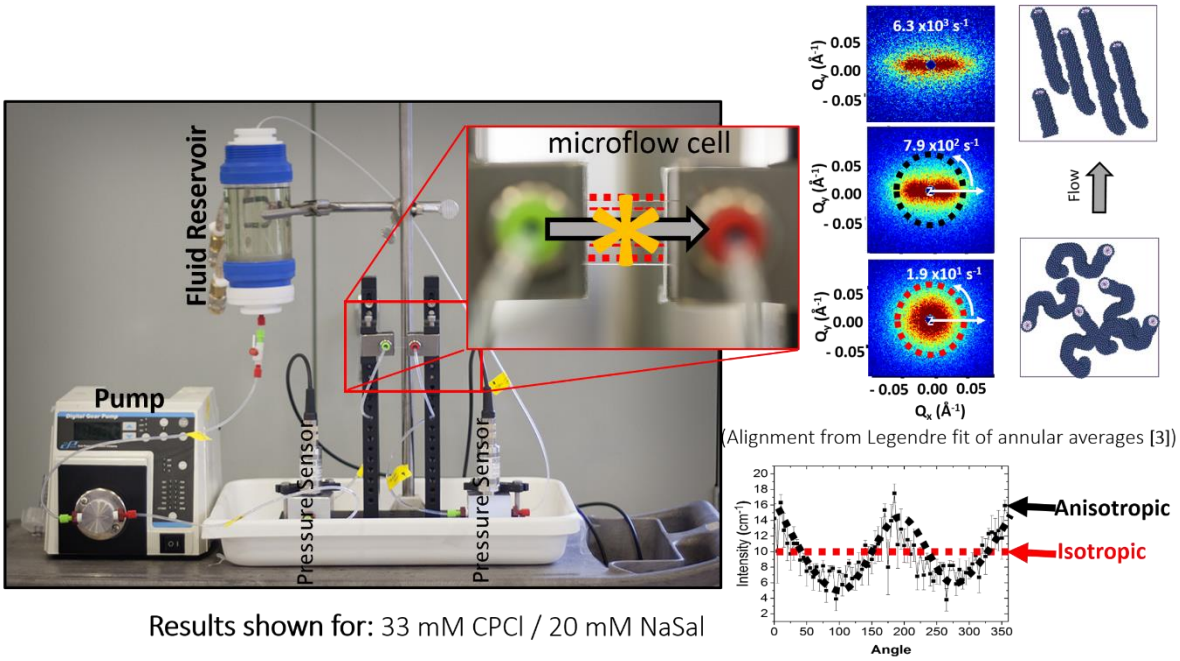

Figure 3: A microfluidic slit rheometer has been designed in order to make simultaneous measurements of rheology and structure at extremely high (> 250,000 s-1) shear rates.

or polymer extruders. These types of conditions can generate levels of shear far greater than those that can be measured in traditional rotational rheometers.

At low flowrates the µRheoSANS technique probes shear rates that overlap traditional RheoSANS measurements. At high flow rates, shear rates orders of magnitude greater than probed with traditional RheoSANS can be accessed. Furthermore, the technique remains a rheoSANS style measurement as rheological data is simultaneously measured in the form a system pressure drop (Fig 3).

Slit Rheometer Basics

A rheometer is any device that can be used to measure how a fluid flows when force applied in a controlled manner. The flow cell apparatus used to conduct µRheoSANS experiments can be used as a slit-type rheometer and provide simultaneous measurement of rheological and structural properties of a fluid. Slit rheometers are used to measure the flow properties of fluid by pumping it through a rectangular channel of known dimensions while measuring both the flow rate (Q) and the change in pressure over the length of the channel (ΔP). These two values can then be used to calculate the stress (τ) and shear rate (γ̇) at the wall of the channel and, finally, the fluid viscosity (η) using the relationships:

$$\tau_{wall} = \frac{\Delta PH}{2L} \quad \text{Eqn. 2a} \qquad \dot{\gamma}_{wall} = \frac{6Q}{WH^2} \quad \text{Eqn. 2b} \qquad \eta = \frac{\tau}{\dot{\gamma}} \quad \text{Eqn. 2c}$$

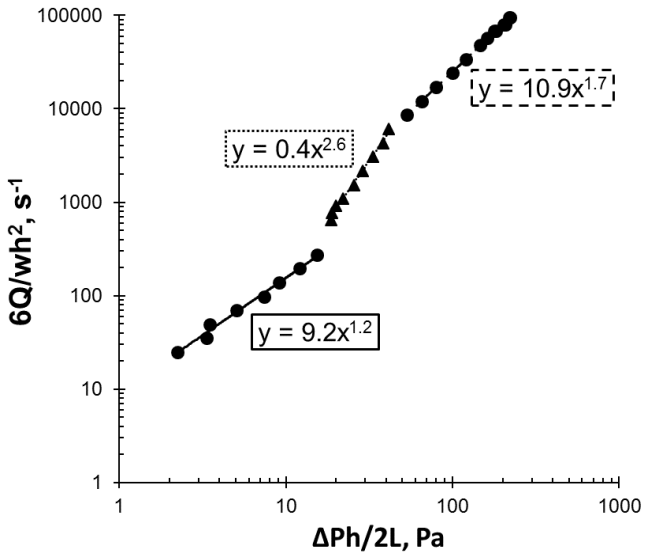

Figure 4: Example plot for making Weissenberg-Rabinowitsch correction for non-parabolic velocity profile

where H, W, and L are the height, width, and length of the channel, respectively and assuming W>>H. The above relationships for shear rate and viscosity require the flow to be laminar and the fluid to be Newtonian (viscosity does not change with shear rate). If the fluid is non-Newtonian, the fluid's velocity profile will be non-parabolic and the true shear rate will deviate from the

apparent shear rate calculated using Eqn. 2b. The deviation from Newtonian behavior is accounted for using a correction developed by Weissenberg and Rabinowitsch (W-R), by plotting wall stress ($\Delta PH/2L$) vs. apparent shear rate ($6Q/WH^2$) on a log-log plot and calculating the slope (see Figure 1). When plotted in this manner, a Newtonian fluid will have a power-law slope of 1, shear-thinning fluids will have a slope >1, and shear-thickening fluids will have a slope <1. The measured slope is then used to calculate the true shear rate ($\dot{\gamma}_t$) from the apparent shear rate ($\dot{\gamma}_a$) using the equation:

$$\dot{\gamma}_t = \dot{\gamma}_a \left(\frac{1}{3} \left(2 + \frac{d\, log(\dot{\gamma}_a)}{d\, \log(\tau)} \right) \right) \quad \text{Eqn. 3}$$

Depending on the behavior of the fluid and the range of shear rates probed, the value used for $d\log(\dot{\gamma}_a)/d\log(\tau)$ could be constant, vary continuously from point to point, or have a series of different values in different shear rate ranges. For example, the data shown in Figure 1 indicates that the fluid is shear-thinning over the entire range of measured shear rates, but has three distinct

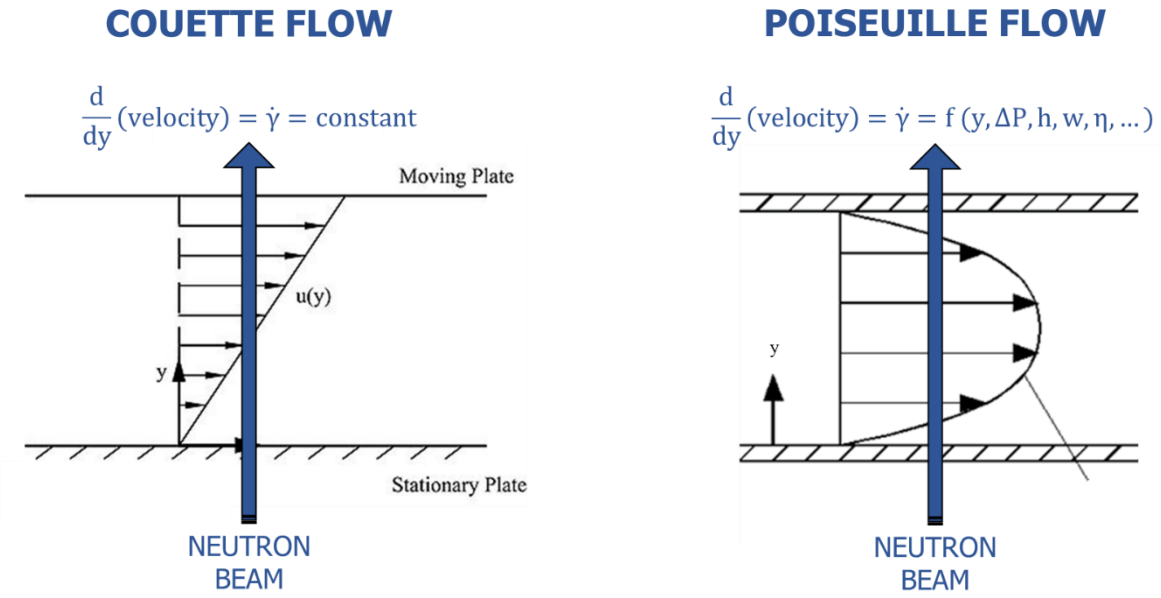

Figure 6: Illustration showing how the velocity and shear profiles generated by sliding plate and pressure-driven flow differ.

regimes: for stresses of 2-15 Pa the W-R correction factor is 1.2, from 20-40 Pa it is 2.6, and from 50-220 Pa it is 1.7. So, when calculating the true shear rate, it is necessary to use each of the three different values in their appropriate stress regimes.

For the μRheoSANS device, in addition to correcting for the non-parabolic velocity profile of non-Newtonian fluids we must also correct for the pressure drop of the tubing and flow adapters connecting the microfluidic flow channel to the inlet and outlet pressure sensors. This is accomplished by using a bypass cell with a flow channel much, much larger than the microfluidic channels, measuring 2 mm x 8 mm x 35 mm. Assuming that the pressure drop over this large channel is negligible, we are able to measure the pressure drop of the tubing and flow adapters as a function of flow rate, and this information is used to calculate the pressure drop over *only* the

microfluidic channel by subtracting the tubing pressure drop from the measured pressure drop during an experiment: $\Delta P_{channel} = \Delta P_{measured} - \Delta P_{tubing}$. Representative pressure drop vs flow rate data for a series of different flow cells, along with power law fits, is shown in Figure 2.

In addition to these two corrections, the current µRheoSANS procedure assumes that slip at the wall of the channel can be ignored and that the pressure drop due to entrance and exit effects are negligible compared to the total pressure drop across the microfluidic flow channel.

Advanced SANS Data Analysis

The µRheoSANS device/technique can characterize the structure of complex fluids at extremely high shear rates. However, the fluid velocity profile in the flow channel is not linear. Therefore, the microfluidic channel contains a convolution of different shear rates that vary throughout the channel as a function of depth; creating a convolution of different scattering patterns during a single SANS experiment, as illustrated in Figure 3. Another complicating factor is that most, if not all, of the samples of interest for µRheoSANS have complex, non-Newtonian rheology, making it much more difficult to understand how the shear-rate changes across the channel when compared to a parabolic, Newtonian velocity profile. To deconvolute the scattering patterns obtained from µRheoSANS experiments the first step is to accurately characterize the flow behavior of the test fluid and obtain viscosity vs shear rate data over as wide a range of shear

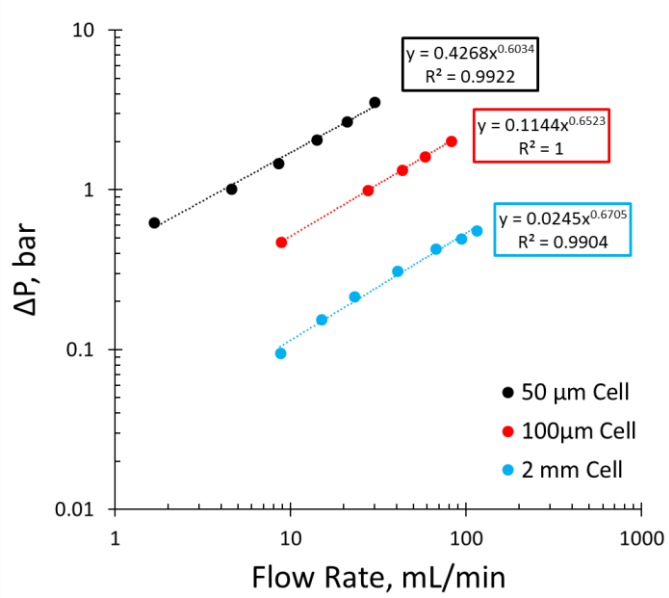

Figure 5: Pressure drop vs flow rate data for three different flow cells. The 2mm cell data is assumed to represent the pressure drop due only to the tubing and flow adapters used by the µRheoSANS apparatus.

rates as possible. This data can then be fit to an appropriate viscosity model (e.g. Carreau-Yasuda, Herschel-Bulkley, Ostwald-de Waele). Velocity and shear profiles for all of the tested flow rates can now be calculated after assuming a linear stress profile within the channel, where the shear stress is zero in the center of the channel and the shear stress at the wall is defined by Eqn. 2a. Given this assumption, it is also true that the shear rate profile for any given flow rate (Q_n), contains the shear rate profile of a lower flow rate (Q_{n-x}) within it since the wall stress varies linearly from

0 to $\tau_{wall,n}$ and $0 < \tau_{wall,n-x} < \tau_{wall,n}$. Additionally, the percentage of the high flow rate condition's shear rate profile containing the shear rate profile at the lower flow rate can be easily calculated from the ratio of the wall stresses. This 'overlap percentage' can then be used to isolate the scattering pattern of the sample in the high shear region near the wall where the two shear rate profiles differ by completing a pixel-by-pixel subtraction of the scaled scattering intensity, as shown in Eqn. 4. In this equation, we first multiply the scattering intensity at a

$$I_{q_x,q_y}(wall) = \frac{1}{1-\frac{\tau_{wall,n-x}}{\tau_{wall,n}}}\left[I_{q_x,q_y}(Q_n) - \frac{\tau_{wall,n-x}}{\tau_{wall,n}} I_{q_x,q_y}(Q_{n-1})\right] \quad \text{Eqn. 4}$$

particular coordinate on the 2D SANS pattern of the lower flow rate, $I_{qx,qy}(Q_{n-1})$, by the 'overlap percentage' and then subtract it from the scattering intensity at the same q_x and q_y coordinate of the scattering pattern from the higher flow rate, $I_{qx,qy}(Q_n)$. Finally, the scattering intensity is renormalized to absolute scale and stored as the scattering intensity of the wall layer, $I_{qx,qy}(wall)$. An example subtraction using this method is shown in Figure 7. It is important to note that the signal-to-noise ratio of the subtracted scattering pattern is significantly worse than that for either of the two original scattering patterns. This must be taken into account during experimental planning; if you plan to try to isolate the high-shear/near-wall using this subtraction method it is necessary to run your scattering experiments for 4-6 times the amount of counts when compared to a standard SANS experiment.

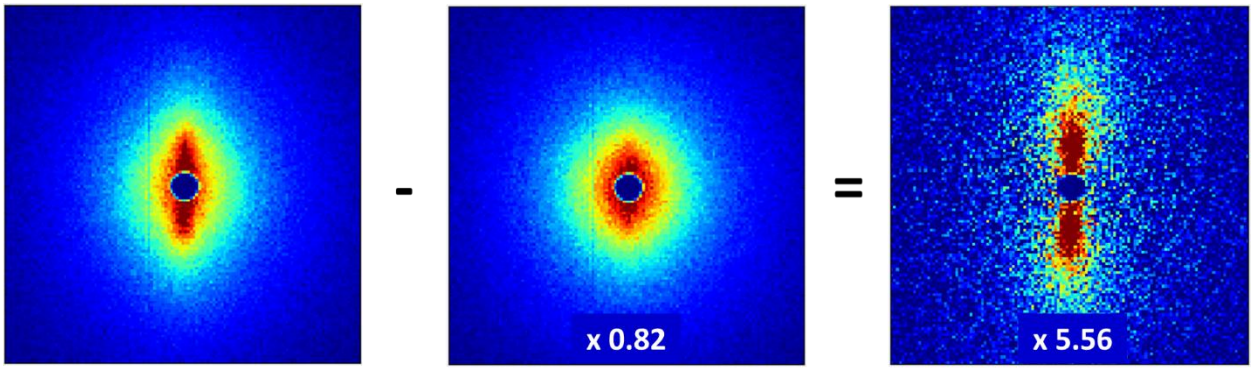

Figure 7: Example subtraction at an intermediate wall shear rate. As expected, the scattering pattern corresponding to the near-wall layer is significantly more anisotropic than either of the convoluted parent scattering patterns. The subtracted scattering also has significantly worse signal-to-noise, an important consideration to keep in mind during experimental planning.

References

1. Yang, J. *Current Opinion in Colloid & Interface Science.* **7**, 276-281 (2002).
2. Hunieda, H.; Acharya, D. P. *Advances in Colloid and Interface Science*. 123-126, 401-413 (2006).
3. Rogers, S. A.; Calabrese, M. A.; Wagner, N. J. *Current Opinion in Colloid and Interface Science-Rheology.* (2014).
4. B. Hammouda, *Probing Nanoscale Structures - The SANS Toolbox, National Institute of Standards and Technology*

5. M.W. Liberatore, F. Nettesheim, N.J. Wagner, and L.Porcar. *Spatially resolved small-angle neutron scattering in the 1-2 plane: A study of shear-induced phase-separating wormlike micelles.* Phys. Rev. E 2006
6. L. Porcar, D. Pozzo, G. Langenbucher, J. Moyer, P.D. Butler. *Rheo-small-angle neutron scattering at the National Institute of Standards and Technology Center for Neutron Research*. J. Rev. Instrum. 2011